Fewer Samples for a Longer Life Span: Towards Long-Term Wearable PPG Analysis

Florian Wolling
Ubiquitous Computing, University of Siegen
Siegen, North Rhine-Westphalia, Germany
florian.wolling@uni-siegen.de

Kristof Van Laerhoven
Ubiquitous Computing, University of Siegen
Siegen, North Rhine-Westphalia, Germany
kvl@eti.uni-siegen.de

ABSTRACT

Photoplethysmography (PPG) sensors have become a prevalent feature included in current wearables, as the cost and size of current PPG modules have dropped significantly. Research in the analysis of PPG data has recently expanded beyond the fast and accurate characterization of heart rate, into the adaptive handling of artifacts within the signal and even the capturing of respiration rate. In this paper, we instead explore using state-of-the-art PPG sensor modules for long-term wearable deployment and the observation of trends over minutes, rather than seconds. By focusing specifically on lowering the sampling rate and via analysis of the spectrum of frequencies alone, our approach minimizes the costly illumination-based sensing and can be used to detect the dominant frequencies of heart rate and respiration rate, but also enables to infer on activity of the sympathetic nervous system. We show in two experiments that such detections and measurements can still be achieved at low sampling rates down to 10 Hz, within a power-efficient platform. This approach enables miniature sensor designs that monitor average heart rate, respiration rate, and sympathetic nerve activity over longer stretches of time.

CCS CONCEPTS

• **Human-centered computing** → **Ubiquitous and mobile devices**; • **Applied computing** → *Health informatics*;

KEYWORDS

Photoplethysmography, sampling rate, frequency spectrum, ambulatory assessment, heart rate, heart rate variability, respiration rate, sympathetic nerve activity

iWOAR '18, September 20–21, 2018, Berlin, Germany

ACM ISBN 978-1-4503-6487-4/18/09…$15.00
https://doi.org/10.1145/3266157.3266209

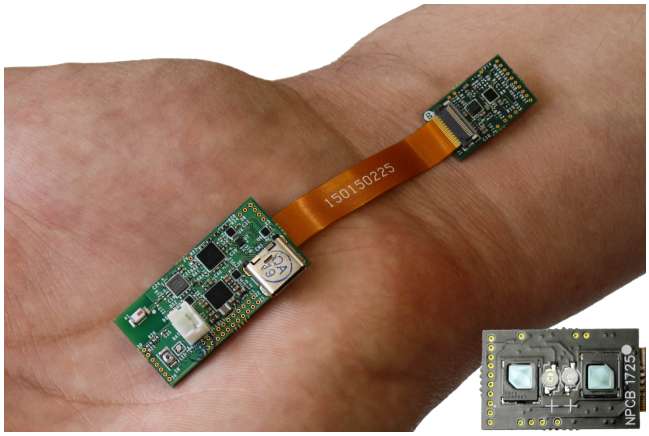

Figure 1: The utilized wearable PPG sensor module uses the *MAX86140/41* evaluation board, which combines a low-power microcontroller, a Bluetooth LE transceiver, and a sensing unit with two photodiodes, a green, and a yellow LED (bottom right). The sensor unit faces the skin surface to measure the scattering light, to infer the blood volume changes in the microvascular bed of tissue beneath the skin.

ACM Reference Format:
Florian Wolling and Kristof Van Laerhoven. 2018. Fewer Samples for a Longer Life Span: Towards Long-Term Wearable PPG Analysis. In *5th international Workshop on Sensor-based Activity Recognition and Interaction (iWOAR '18), September 20–21, 2018, Berlin, Germany.* ACM, New York, NY, USA, 10 pages. https://doi.org/10.1145/3266157.3266209

1 INTRODUCTION

Wearable monitoring of heart rate has surged in the past decade, allowing more representative 'in vivo' observations in the user's natural surroundings. With the advance of photoplethysmography (PPG) sensor units in smartwatches and other wearables, such sensor units have become smaller, less invasive, and more comfortable to attach to the body. Due to the optical measurement principle, these PPG sensors do not require perfect attachment of electrodes on the skin, though their data are known to suffer from ambient light and changes through motion or pressure on the skin. Furthermore, their reliance on high-intensity LEDs to illuminate

the skin is far from energy-efficient, hindering lightweight and wearable deployment for extended periods of time.

Current research in PPG is targeting in particular the accurate detection and segmentation of pulses for heart rate (HR) measurement and the extraction of the related heart rate variability (HRV). The determination of this parameter even enables to estimate the respiration rate (RSP) in terms of its frequency, intensity, and amplitude. The aim of most studies is to deliver results that approach the accuracy and speed of electrocardiography (ECG) and clinical respiration monitors, which represent the reference signals for HR and RSP parameters. Consequently, most approaches use high sampling rates (SR) for a better temporal resolution, although those do not lead to significant benefits regarding accuracy, but increase the energy consumption of the system.

In this paper, we argue for using a wearable PPG sensor for observing *slower trends*, across longer stretches of time, by evaluating data that span minutes rather than seconds. Using spectral analysis of minute-long signals, our aim is to extract the different oscillations present in the PPG signal that correspond to heart rate (HR), respiration rate (RSP), and a third range which has been identified to represent sympathetic nerve activity (SNA). We specifically investigate how the PPG sensor's sampling frequency (SR) will affect such estimates, since the LED-driven measurements are a major hurdle for wearable deployments.

Our aim is, thus, to focus specifically on obtaining correct estimates for average physiological signals, efficiently measurable with a small and wearable PPG sensor. Hence, we are aiming for the application of unobtrusive devices such as smart patches, to record measurements in long-term studies.

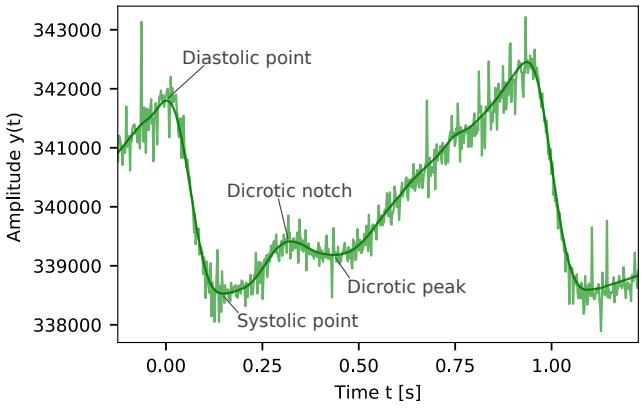

Figure 2: The PPG signal of a single cardiac cycle, measured with green light at 512 Hz sampling rate, showing mirrored run due to reflective measurement principle. Note the characteristic features, diastolic and systolic point, dicrotic notch and peak of reflected wave from lower extremities and aorta, as well as the spikes of interfering noise.

The importance of observing large time windows of PPG data is increased by recent commercial PPG sensors, which optimize the timing of the sensors' LEDs exposure considerably and as such enable sparse, and as a consequence energy-efficient, data sampling. To illustrate our approach, we present a prototype design that integrates such a recent PPG sensor based on the *MAX86140/41* in a microcontroller-driven evaluation system, and demonstrate the impact of the sampling rate on its overall power efficiency.

This paper's contributions are threefold:

- Spectral analysis over minute-long data is detailed as a promising wearable method to estimate heart rate and respiration rate, as well as the presence of sympathetic nervous activity. It is limited to estimating averages over minutes, but works on low sampling rates, allowing long-term operation on light-weight devices.
- We present a first study on a 42-person benchmark dataset, in which the impact of the sampling rate of PPG data is evaluated on the accuracy of the estimation of heart rate, respiration rate, and sympathetic nervous activity.
- We present a second study on data from a wearable prototype using a novel low-power PPG sensor, showing the specific advantages of our approach over larger windows of lower-frequency PPG samples.

The remainder of our paper is structured as follows: We start with presenting the background concepts of photoplethysmography (PPG) and related work on estimating parameters such as heart rate (HR), respiration rate (RSP), and the presence of sympathetic nerve activity (SNA). A wearable PPG system design is then presented, which uses a recent integrated PPG sensor and a low-power microcontroller to illustrate the effects of our proposed method on an actual system. After proving details on our signal analysis approach, we present two studies: One on a clinical benchmark dataset of 42 individuals and a second study with 6 individuals taken with the presented wearable PPG system. We conclude with the results from these studies, as well as several observations made during the second study.

2 THEORY AND RELATED WORK

Before we specify the design of our wearable PPG sensor on the hardware level, we first present related work and introduce into the theoretical concepts and mechanisms of photoplethysmography (PPG), the determination of heart rate (HR) and respiration rate (RSP), the identification of activity in the sympathetic nervous system (SNA), and the central issue of the sampling rate (SR).

Photoplethysmography

Pulse oximetry is a proven and tested method in clinical settings, where it is used to non-invasively obtain heart rate (HR) and peripheral oxygen saturation (SpO_2) of patients. It is based on photoplethysmography (PPG), an optical principle for the measurement of blood volume changes in the microvascular bed of tissue beneath the skin. In the traditional setup, an LED emits light into the skin which is then measured on the opposite side of the tissues. Consequently, the measure represents the amount of light that has not been absorbed within. Instead of a clip at the fingertip, typical for this transmission measurement, modern wearables use a variation of this method in which LED and photodiode are placed close to each other, on a single side. Thus, not the absorption, but the scattering of light within the tissues is measured at the skin surface. Consequently, the signal sequences of the principles show a mirrored run and the systolic peak being either the maximum for the transmissive or, as depicted in Figure 2, the minimum for the reflective principle. While the signal of transmissive PPG is proportional to the detected blood volume, the one of the reflective PPG shows an antiproportional signal sequence due to a larger blood volume that is absorbing the emitted light [10].

Depending on the light's wavelength, variations in different layers of the tissue are captured: Blue and green light measure the blood volume changes in the superficial capillaries of the uppermost epidermis, yellow reaches the arterioles in the dermis, and red or infra-red even reach the small arteries in the hypodermis [1, 13]. In contrast to the arteries and arterioles, veins do not exhibit observable changes in blood flow and, just like other passive tissues, add another DC component to the detected signal.

Determined by the systolic and diastolic phase of the cardiac cycle, the heart generates a pulse wave that travels through the body as a difference in blood pressure and volume. This is, therefore, measurable with PPG and enables the estimation of HR by identifying and counting the average pulse beats per minute. Due to the loose deployment of the sensors on the user's skin, artifacts from motion and differences in pressure can be expected in long-term 'in vivo' measurements, making the reliable measurement more challenging. However, as summarized in [16], research already showed successful approaches to identify artifacts and to minimize their influence [6, 11].

Heart Rate and Respiration Rate

Initially, PPG sensors have been utilized to just measure the pulse beats and, thus, to infer HR by counting the peaks and averaging their quantity over one-minute intervals. Research then focused on minimizing the influence of motion artifacts to make the measurements increasingly reliable. Apart from algorithms which improve the robustness of heart beat detection, research is recently aiming for extracting further information from PPG signals. Besides the estimation of the peripheral oxygen saturation (SpO_2), recently the estimation of the respiration rate (RSP) has been spotlighted.

On the one hand, breathing results in fluctuations of the blood pressure, the so-called respiratory-induced intensity variation (RIIV), which volume changes are observable in PPG signals as an oscillation at the RSP frequency. On the other hand, respiration appears as slight variations in heart beat distance, the so-called respiratory sinus arrhythmia (RSA). The phenomenon is observable at every living individual and is not subject to diseases. While it is also referred as respiratory-induced frequency variation (RIFV), the more common name heart rate variability (HRV) just describes the varying time intervals between consecutive pulse peaks. Although the parameter is of interest for the medical diagnose of diseases [14], in research for wearable devices the next stage still focuses on its use for the reliable estimation of RSP [2–4, 8]. Because the signal amplitude of PPG signals is more interfered by baseline wandering and motion artifacts, to date, HRV prevailed as a reliable measure of RSP due to those interferences having less impact as long as the peaks are effectively detected and located.

Sympathetic Nerve Activity

The autonomic nervous system of the human consists of two parts which regulate the body's unconscious activity and act complementary to each other. While the parasympathetic nervous system with a slower response controls the body at rest and is responsible for the *rest and digest*, the sympathetic nervous system with a faster response controls the shortening reactions of *fight or flight* in case of a threat.

As one of the major problems of today's society is suggested to be constant stress of its individuals, resulting in an outbalance of the sympathetic part, the examination of this development is more important than ever. The sympathetic nerve activity (SNA) plays a crucial role in the monitoring of cardiovascular diseases such as hypertension, heart attacks, cardiac arrhythmia, and congestive heart failure. Though, the explicit measurement of the SNA is difficult, because only its consequences, such as a constantly higher HR or a permanently increased sweating, are observable without complex medical equipment. Hence, a method to explicitly measure SNA, embedded into small and light-weight wearable devices, would be highly beneficial to observe stress in large-scale and long-term studies.

Fortunately, the presence and amplitude of low-frequency oscillations in the arterial blood pressure, spontaneously occurring in conscious humans, have been shown to correlate with SNA [15]. In this way, the SNA is likely observable in unfiltered measurements of present PPG sensors, but needs further investigation to be well-understood.

Sampling Rate

The temporal resolution of a PPG measuring sequence is dictated by its sampling rate (SR), represented by the number of emitted flashes that are scattered within the tissue and, finally, detected by a photodiode. The trend to inconsiderately increase this SR frequency prevailed for a while. On the one hand, it has been motivated by the filter-based stabilization of the average which statistically represents the expected value, smooths the slope, and thus suppresses occurring noise. On the other hand, the interpretation of the heart rate variability (HRV) requires a higher SR to precisely locate the pulse peaks and to measure the difference in time interval between consecutive peaks. Figure 3 illustrates the relation between the SR and the temporal resolution which is required for an accurate HRV estimation.

Due to the high energy consumption and the desire of small and long-lasting wearable devices, research again concentrates on the reduction of the SR, to reach its necessary minimum. Thus, the fundamental sampling theorem of Nyquist-Shannon returns to mind, which defines the possible minimum SR that is necessary to reliably capture the desired signal frequency. However, in the raw measurement data, the interfering noise is not filtered and thus not band-limited. Consequently, a higher SR is required to still correspond to the guideline of the sampling theorem. However, at a certain point, the benefits of a higher SR stagnate while the energy consumption still increases constantly.

In their approach, De Giovanni et al. [7] examined the energy-efficient estimation of HR based on a single-sided amplitude spectrum analysis, applying the FFT on short windows of PPG data. The algorithm removed the existing motion artifacts without the reconstruction of a noise-free signal or adaptive filtering. Additionally, by lowering the SR from 125 Hz to 31.5 Hz they were able to reduce the required memory to 5.8 kB. At the same time, the average absolute error increased only from (1.27 ± 0.91) bpm to (2.24 ± 1.01) bpm.

A similar approach has been examined by Choi et al. [5] which evaluated the required minimum SR to reliably analyze the HRV. The original 10 kHz PPG signal has been sampled down to the range of 5 kHz to 5 Hz. Afterwards, the signal sequences have been analyzed in time and frequency domain, and then compared to the reference ECG measurements with a SR of 10 kHz. As a result, it is stated that a SR beyond 25 Hz does not show significant difference to the lower ones and, thus, higher SRs do not contribute to the reliability of PPG for the HRV estimation.

3 WEARABLE PROTOTYPE

For the practical evaluation of our approach, we decided to use the *MAX86140/41* and its evaluation board as an integrated optical data acquisition system. It is a state-of-the-art low-power platform that is suitable as a light-weight and wearable PPG-sensing system, presented in Figure 1.

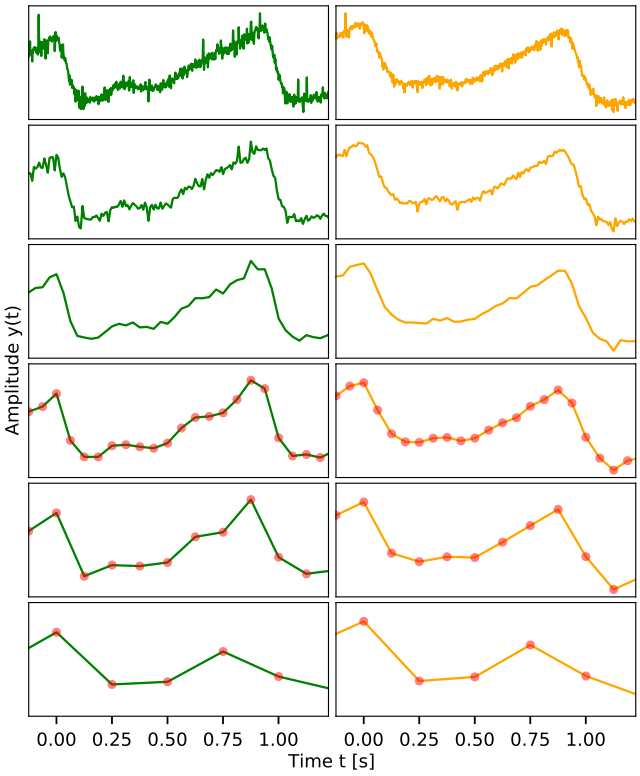

Figure 3: Illustration of downsampling of the original PPG signal sequences, with the channels of green light (left) and yellow light (right), from 512 Hz (top) down to 128, 32, 16, 8, and 4 Hz (bottom). With lower frequency, the temporal resolution decreases and an accurate localization of the pulse peaks is not possible anymore.

Its central microcontroller is a *MAX 32620* ARM Cortex-M4 with floating point unit. It includes 2 MB of flash memory and 256 kB of SRAM to collect the measurements. Readings can also be transmitted via the *nRF52832* Bluetooth LE transceiver for intermittent further processing and long-term offline storage. The *MAX86140* itself provides three programmable 8 bit LED driver DACs for pulse modulation and a low-noise analog front-end (AFE) with a single input channel to a 19 bit sigma-delta ADC with integrated filter for 50 and 60 Hz interference. It provides sampling rates (SR) from 4096 Hz down to 8 Hz. Furthermore, the manual triggering enables individual sequences, even lower than 8 Hz. The option of using a low SR in combination with diverse energy saving modes and a proximity function to detect skin contact enables the use of this hardware design in low power applications such as ours. The influence of ambient light is compensated and abrupt changes can be rejected by a picket fence detect and replace algorithm for value estimation.

As a result, the modules provide stable signals, but still allow to obtain unfiltered, raw PPG measurements. Those enable the unconstrained offline analysis of recorded signals, including the application of possible filters without anticipating the necessity of preprocessing stages such as a low-pass filter for the elimination of baseline wandering.

Essential for the PPG measurement is the selection of a suitable light source. Due to blood's absorption characteristic, green and yellow visible light spectrum exhibits the largest modulation depth in the detected signal and, hence, provide the best signal-to-noise ratio [16]. The prototype provides a green LED (*LT PWSG*) with $\lambda_g = 528\,\text{nm}$ and a yellow, amber-colored LED (*LY P47F*) with $\lambda_y = 590\,\text{nm}$. To detect the small variations of the scattered light, the system utilizes two photodiodes (*VEMD5010X01*) with a sensitivity suitable for visible and near infrared light.

In our experiments, we decided for the following measuring parameters: During each sample, the LEDs are successively turned on, driven with a current of 4.9 mA. After a settling time of 12 µs the reflected light is integrated for 14.8 µs and, finally, measured by the ADC. Although the measurement time can be extended up to 117.3 µs, resulting in a higher signal-to-noise ratio, we decided for the described default configuration due to a significant lower energy consumption, nevertheless, still providing a sufficient modulation depth for most skin types.

However, the duty time of 14.8 µs already results in a time-averaged current of 262.64 $\frac{\text{nA}}{\text{Hz}}$. Thus, the activation of each discrete LED incorporates a relevant portion of the prototype's energy consumption: 1.076 mA at 4096 sps; 134.5 µA at 512 sps; 16.8 µA at 64 sps; 2.1 µA at 8 sps. Though, not only the LEDs' demand increases linearly with the applied SR frequency, also the analog front-end (AFE) consumes a rising current, ranging from a few µA up to about 1170 µA. So just the PPG module's sensor front-end with a single LED consumes about 2 mA at the maximum SR of 4096 sps, compared to less than 5 µA at about 10 sps. In addition, a higher SR has large impact on the microcontroller's busyness, resource and memory usage, again resulting in a larger dissipation.

4 EXPERIMENT I: PPG ANALYSIS ON A PUBLIC DATASET

To evaluate our approach, we first validated our assumption regarding the effect of SR on spectral analysis of PPG data with a publicly available dataset that has been recorded from a highly variable set of 42 users.

Although numerous public datasets for HR estimation from electrocardiograms (ECG) are available in databases like the PhysioBank [9] repository, raw photoplethysmography (PPG) data is not as easily found. We used the IEEE TBME benchmark dataset based on the CapnoBase database as presented and described in [12]. It is one of the few publicly available clinical datasets that contains synchronized ECG, PPG, and respiratory CO_2 recordings from a large variety of persons. The dataset was originally devised for examining RSP estimation algorithms from raw PPG signals for 42 persons, for a duration of eight minutes each and sampled at 300 Hz. The PPG readings are complemented with reference CO_2 readings, ECG readings, and artifact labels validated by an expert rater. Figure 4 shows a one-minute segment of raw ECG, CO_2 RSP, and PPG data from this repository, and our frequency analysis for the said segment.

In a first pass, possible artifacts in the dataset are eliminated by selecting, for each person, a one-minute subset of data for which no artifacts are present in the ECG, CO_2, or PPG signals. These artifacts are annotated in the benchmark, using the Incremental-Merge Segmentation algorithm [11], which detects short-term artifacts by identifying abnormally large and clipped pulses. Subsequently, the DC component in raw PPG data is removed through a high-pass filter with

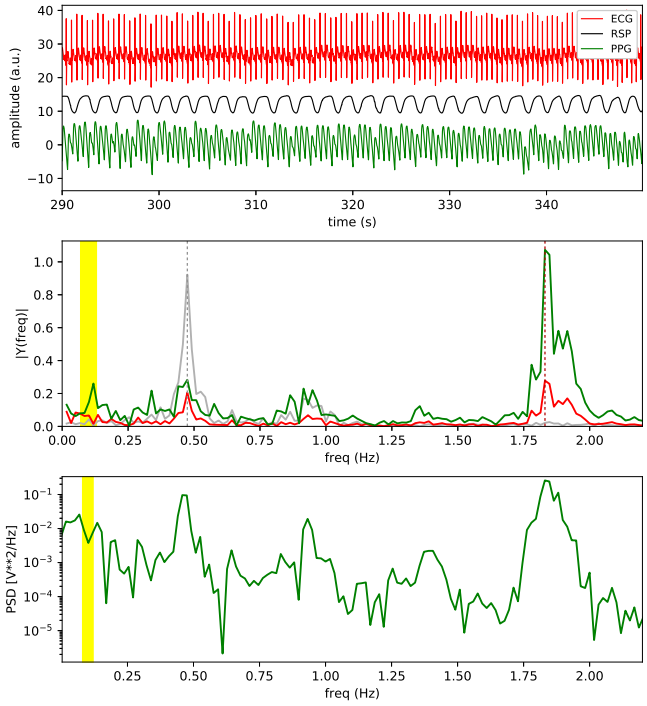

Figure 4: Analysis of an excerpt from the benchmark study [12] taken from 42 individuals. Top: Original time-series over minute from wearable ECG, respiration (CO_2), and PPG sensors, all sampled at 300 Hz. Middle: Frequency spectrum of PPG data (green), annotated with frequencies and dominant frequency in heart rate (red) and respiration (grey) from the ECG and CO_2 data respectively. Occurrence of low-frequency processes typical for sympathetic nerve activity. Bottom: Power spectral density plot of PPG data with default parameters for a Welch periodogram.

a cutoff frequency of 0.01 Hz. Spectral analyses is performed using the Welch averaged periodogram method: The PPG timeseries are divided into 50 % overlapping 60 s segments, computing a modified periodogram for each segment, and averaging the resulting periodograms. The segments are Hanning-windowed, to minimize the first sidelobe of the frequency response, and Fourier transformed using FFT. The range of the expected RSP and HR frequencies is as in [12] defined as 0.067-1.08 Hz or 4-65 cpm for RSP and for the HR a similar search window that reaches up to 3 Hz or 180 cpm. For the calculation of the average frequencies for both HR and RSP, the frequencies with maximum power within the respective ranges are then identified. For SNA, the area under the power spectrum is computed for the low frequency range from 0.04 to 0.15 Hz [2].

To study the effect of the SR of PPG on the detection of HR, RSP, and SNA, we systematically removed intermittent samples from the original 300 Hz data, down to 2 Hz. Figure 5 shows the results for the recovery HR and RSP, using a range of distance thresholds from 0.005 Hz up to 0.1 Hz. The predicted frequency is marked as correct if it is within this threshold from the ground truth, and false otherwise. Overall, the detection of the RSP around 80 % is lower than the HR around 90 % for the same thresholds. The detection for the HR and RSP accuracy can also be seen to deteriorate rapidly after reducing the SR to 4 Hz.

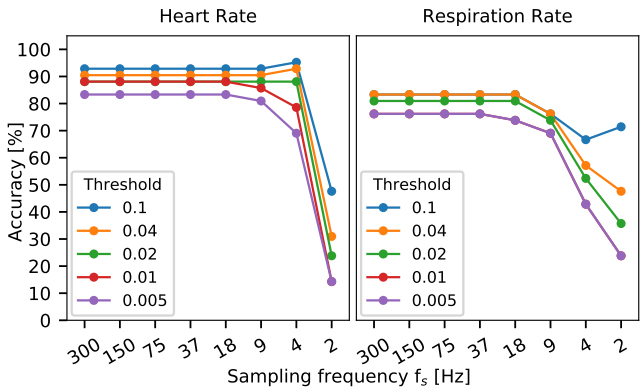

Figure 5: Accuracy for the detection of respiration rate (left) and heart rate (right) from the PPG readings, while varying the sampling rate from the sensor's original 300 Hz down to 2 Hz. The different lines represent the results using different thresholds to establish whether a correct prediction was made. They are measured in Hz as the maximum absolute distance between prediction and ground truth. Note that reducing the sampling rate to as low as 18 Hz or 9 Hz has a moderate to minor effect, with a more severe impact for the estimates of the respiration rate.

5 EXPERIMENT II: PPG ANALYSIS ON EXPERIMENTAL DATA

After the basic evaluation of our approach, based on a publicly available PPG dataset, in a second experiment, we analyzed and evaluated experimental data from the previously presented wearable PPG sensor system.

Experimental Setup

For the experiments, besides the PPG sensors themselves also other sensors have been utilized to provide ground truth information about the actual RSP, but also to detect mechanical disturbances. The recordings have been analyzed offline on a computer. To provide a matched data base, the sensors have been synchronized with specific gestures.

Applied Sensors. Primary device is the previously presented wearable sensor module based on the *MAX86140/41* that has been utilized to record raw PPG data at the right wrist. This position has been chosen, because it is the most common position for wearable devices such as fitness trackers and it is usually perceived as rather unobtrusive. Further, we employed the onboard accelerometer *BMA280* to support the identification of occurring disturbances. Besides the elimination of motion artifacts, this even enabled to examine the mechanical influence of breathing, as the arm is slightly displaced with every thorax movement. To gather ground truth information about RSP, a secondary sensor module has been attached below the chest's left pectoral muscle, close to the heart. It focuses on the acceleration that is changing due to the direct thorax expansion and, consequently, enables to infer the RSP. The position has been chosen to additionally test the PPG principle at this position in foresight for the use in smart patches. However, the chest strap of the secondary device has been perceived as unhandy and uncomfortable, and was not applied in later study experiments. Instead, a time-of-flight (ToF) depth camera has been utilized to remotely measure the respiratory movements of the thorax. This measurement principle has been validated in detailed respiratory experiments and showed high accuracy and reliability (see Figure 6). The two wearable modules recorded the measurements of the two PPG channels, green and yellow light, the ambient light intensity, and the acceleration in three axes at a SR of 512 Hz. For both PPG channels, the influence of ambient light has automatically been detracted. Due to the slower frame rate of the depth camera, the RSP reference signal is recorded at about 30 Hz.

Synchronization. The PPG sensors and accelerometers are synchronized onboard. However, the two wearable devices, attached to wrist and chest, as well as the external depth camera still have to be synchronized among each other. To link the wearable modules, their casings are tapped against each other to generate significant peaks in the acceleration. Subsequently, a fast waving gesture, of the arm with attached

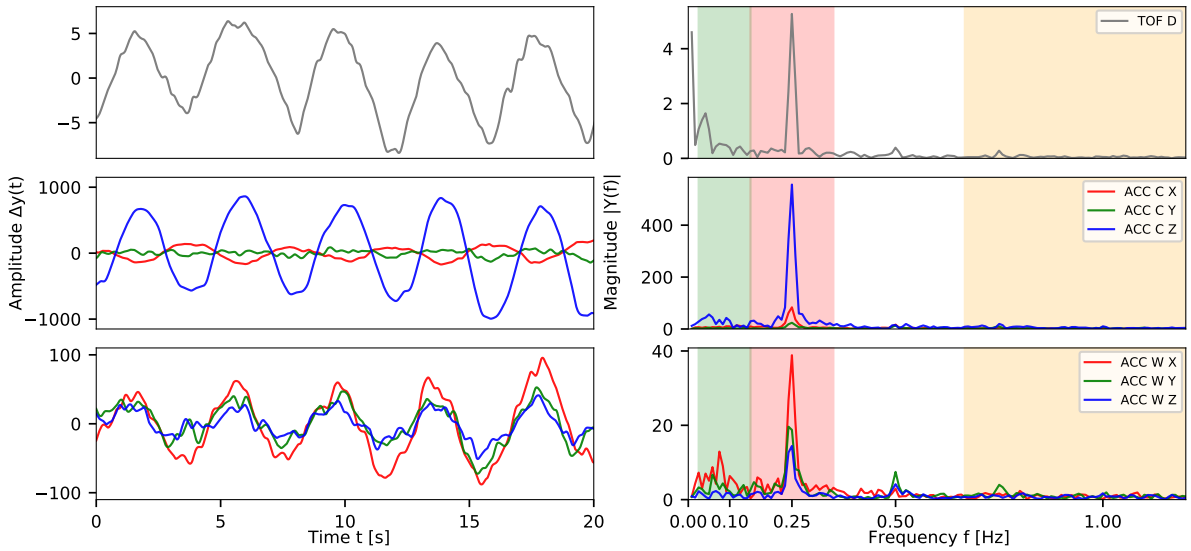

Figure 6: Validation of paced breathing at 0.25 Hz (15 cpm). Measurement of thorax expansion with ToF depth camera (top), accelerometer at the chest (middle), and accelerometer at the wrist (bottom). Time series segment of 20 s (left) and frequency spectra of full 120 s recordings (right). Depth camera band-pass filtered in time series 0.5 Hz to 50.0 Hz and unfiltered in frequency spectrum. Acceleration data band-pass filtered from 0.025 Hz to 2.0 Hz in both cases.

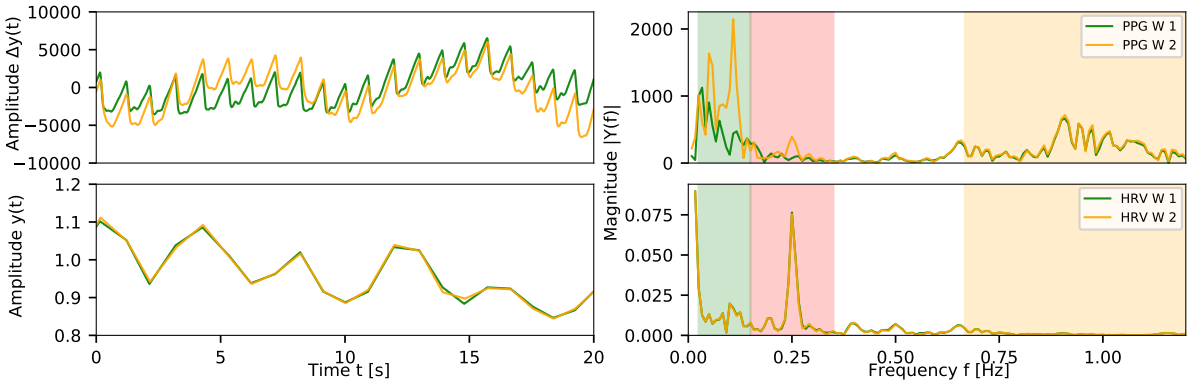

Figure 7: Analysis of PPG data at the wrist during paced breathing. Time series of 20 s raw PPG data (top left), frequency spectrum of full 120 s raw data (top right), linear interpolated HRV from irregularly sampled maximum peak-features (bottom left), and respective frequency spectrum (bottom right). Top right: Significant SNA (green area), observable RSP (red area), and HR (yellow area). Bottom right: Significant RSP (red area).

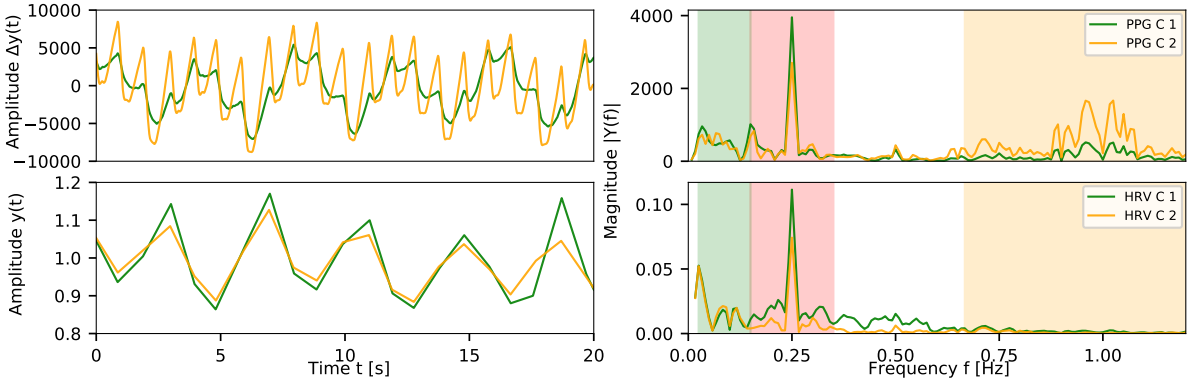

Figure 8: Analysis of PPG data at the chest during paced breathing. Time series of 20 s raw PPG data (top left), frequency spectrum of full 120 s raw data (top right), linear interpolated HRV from irregularly sampled maximum peak-features (bottom left), and respective frequency spectrum (bottom right). Top right: Observable SNA (green), significant RSP (red), and HR (yellow). Bottom right: Significant RSP (red).

sensor module, through the measurement window, spanning the chest of the detected subject, enables to link the depth camera signals with the acceleration of the wearables. By executing this procedure at the beginning and the end of the recordings, also the clock drift of the particular devices can be rectified which is important for longer time spans. Unfortunately, the PPG pulse signals themselves are inapplicable to synchronize the wearable sensor modules. The mechanical propagation of the pulse wave through the arteries is too slow and would result in a considerable inaccuracy due to a noticeable difference in time of arrival (ToA).

Applied Filters and Algorithms

Hereafter, the applied filters and algorithms are described which have been utilized to extract the desired parameters HR, RSP, and SNA from the recorded signals. At first, the parameters are estimated regarding the approach of this research, based on the frequency spectra of the fast Fourier transform. Then, those are compared to the estimates that have been extracted on the traditional way, based on established and accepted standard techniques.

Fast Fourier Transform. According to the concept of our approach, the recorded raw measuring sequences of the PPG sensors are converted from time into frequency domain using the fast Fourier transform (FFT) algorithm. Essential for this transformation are the window parameters of time span T and number of samples N, joined in the SR frequency $f_S = \frac{N}{T}$. For a single-sided spectrum, N results in the respective number of bins $\frac{N}{2}$. Those capture a certain frequency range which is defined by the frequency resolution $\Delta f = \frac{f_S}{N}$. However, according to the theorem of Nyquist-Shannon, the covered frequency band cannot exceed $f_{max} = \frac{f_S}{2}$.

While the limit f_{max} does not affect the measured signal frequencies of HR, RSP, and SNA, the resolution Δf is crucial for the accurate estimation of the expected values. Consequently, for a better Δf, the SR has to be increased already in time domain. Though, as the accuracy converges quickly, the improvement of Δf by increasing SR gets negligible soon.

Heart Rate and Peak Position. The most fundamental measurement of PPG is the HR. To extract this parameter from the measured signals, a standard peak detection algorithm has been applied. It is common even though not efficient, but ensures the independency from specific concepts and algorithms. Thus, it returns not only the count of peaks per window length, but also their position which is basic requirement for the subsequent parameters. To achieve a reliable locating of the pule peaks, the algorithm has been configured considering the standard HR frequency range between 0.67 Hz and 3.67 Hz respectively 40 bpm and 220 bpm [7]. Due to optimal conditions of the selected data windows

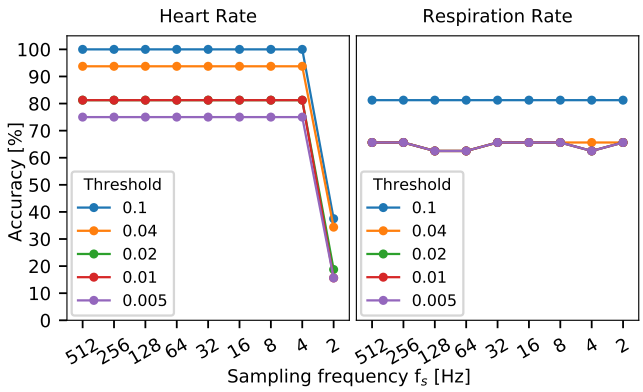

Figure 9: Accuracy for the detection of respiration rate (left) and heart rate (right) from the PPG readings, while varying the sampling rate from the sensor's original 512 Hz down to 2 Hz. The different lines represent the results using different thresholds to establish whether a correct prediction was made. They are measured in Hz as the maximum absolute distance between prediction and ground truth. Note that reducing the sampling rate has only minor effects for respiration rate and a more severe impact for heart rate.

without motion artifacts, this approach is sufficient. Before the peak detection is executed, the signal is filtered with a forward-backward, linear phase, 2nd order band-pass filter to reject baseline wandering and noise below 0.025 Hz and beyond 10.0 Hz. This filtering would not be necessary for the specialized approach of Karlen et al. [11] which is popular for wearable devices and more reliable in real life applications.

Heart Rate Variability and Respiration Rate. Due to respiratory-induced intensity variation (RIIV), it is possible to extract RSP directly from the fluctuations in the raw PPG signals. Though, because this measure is very sensitive to motion artifacts, the measurement of the related phenomenon RSA through HRV is currently the most common way. The slope of HRV is derived from the positions of the pulse peaks which have been used to generate the envelope function of the raw PPG signal. The maxima respetive the diastolic base points represent an irregularly sampled sequence of peak-features that is resampled using linear interpolation [4, 12].

Sympathetic Nerve Activity. For the activity of the sympathetic nervous system, the area under the curve of the frequency spectrum between 0.04 and 0.15 Hz has been computed and compared to those of the other measurements.

6 RESULTS AND DISCUSSION

In the following, we briefly summarize, compare, and discuss the results of the particular experiments.

Experiment 1. A typical time series of the benchmark dataset is shown in Figure 4 and contains the three channels of ECG, RSP CO_2, and PPG. Although the patients did not perform paced breathing at a specified frequency, the respiration signal still shows a uniform, continuous signal and a steep, significant peak in its frequency spectrum. The heart beat is distinctively observable in both, the ECG and the PPG signals. The superimposing respiratory-induced intensity variations (RIIV) are simultaneously observable in both channels, however, their amplitude is clearly lower than the primary pulses. As a result, the frequency and power spectra show significant peaks at the fundamental frequencies of HR and RSP within the mentioned frequency bands. The peak of the RSP CO_2 measurement is congruent with the RSP-associated peaks in the ECG and PPG channels, but those are less distinct. In contrast, the dominant frequency peak of HR is several times larger than the one of RSP due to its smaller amplitude of the superimposing RIIV.

The results of the downsampling are presented in Figure 5 and show a relatively stable accuracy down to about 9 Hz SR for both HR and RSP with about 90 % and 80 % correctly identified dominant frequencies.

Experiment 2. In contrast to the preliminary benchmark study, our subjects performed paced breathing at 0.25 Hz. As is observable in Figure 6, all three reference measurements, either of the time-of-flight (ToF) depth camera or of the onboard accelerometers, show a similar signal, resulting in a significant peak at the desired RSP frequency of the spectra. Thus, the ToF depth camera provides reliable reference measurements and is a valid replacement for the obtrusive chest strap that has been used in the first experiments. Although still observable at the wrist, the influence of the respiratory motion due to thorax displacement is negligible.

The Figures 7 and 8 show exemplary time series of the PPG sensors attached to wrist and chest. Obviously, the chest sensor's signal is considerably superimposed by RIIV. Because the pulse peaks are clearly visible and no harsh motion artifacts are observable, direct mechanical influence of the thorax displacement on the signal can be excluded. In contrast, the PPG signal at the wrist does not contain obvious superimposition from RIIV. Instead, a low frequency component is visible, which is not noticeable at the chest. Analog to the observations in time domain, the frequency spectra of the sensors show significant peaks for RSP at the chest and for low frequencies at the wrist. Both spectra show scattered peaks around the actual HR, though their distributions are neither similar nor comparable in width and shape.

Due to the phenomenon of the respiratory sinus arrhythmia (RSA), the analysis of the feature-based heart rate variability (HRV) reveals the RSP signal at both measurement positions, at the wrist as well as at the chest. Both curves swing around the average inter-beat distance, about 1 s in this case, but exhibit a different phase. The resulting peak of the RSP dominant frequency is significantly observable in both HRV spectra. In contrast, the HR frequency band is not occupied at all. While the spectrum of the wrist's raw data showed a distinct increase within the low frequency range, this frequency band is just unremarkable in the HRV spectra of both sensor positions.

The results of the downsampling are presented in Figure 9 and show a relatively stable accuracy down to about 4 Hz SR for both HR and RSP. The average accuracy spreads around 80 % for HR and 70 % for RSP.

Discussion. Both experiments showed the feasibility of inferring HR and RSP from frequency spectra at reduced SR without losing reliability and accuracy. Of course, the aggregation of the information in a minute-long measurement window and the calculation of its average results in a coarsening, but the resulting resolution is usually sufficient for long-term observations. In general, the RSP frequency can be extracted from both spectra, based on the raw measurements or the HRV information. Instead, the HR itself can only be derived from the raw signal's spectrum. Due to the paced and, therefore, constant RSP frequency in the second study, the dominant frequency was extraordinary significant and easy to extract. Variations in breathing and the change of the fundamental RSP frequency within a measurement window spreads the frequency components and, thus, flattens the peaks. This behavior is observable for HR at which the slight frequency variations of RSA generate a broad distribution with side lobes according to the swing of the HRV signal.

7 CONCLUSIONS

We have presented a method to obtain information through spectral analysis of photoplethysmography (PPG) data, which we argue is particularly suitable for wearable and long-term monitoring as it allows sampling at considerable lower frequencies. The wearer's heart rate (HR) and respiration rate (RSP) are essentially calculated by observing dominant frequencies in their respective frequency bands. Additionally, the activity of the sympathetic nervous system (SNA) is inferred by capturing the area under the curve in the characteristic low frequency band. Although the presented methods do not provide detailed, peak-specific identification and segmentation, which is what many state-of-the-art approaches currently aim for, it does lend itself well for energy-efficient PPG monitoring and solutions that need to be light-weight and wearable over longer stretches of time.

We presented a design around a modern PPG sensing unit to illustrate that, despite several features such as detection of artifacts and motion, the high sampling rates (SR), which are currently common in PPG sensing, represent a considerable bottleneck for such systems. We also show that spectral analysis can be implemented on current systems, as it depends largely on the fast Fourier transform (FFT) to divide a window of PPG data into its frequency components. Even for minutes of data, as required by our method to observe low frequencies of sympathetic nerve activity (SNA), this is achievable in off-the-shelf hardware.

In two studies, we have shown that the PPG sampling rate (SR) can indeed be reduced to 10 Hz, without significant deterioration of the detection performance of heart rate (HR) and respiration rate (RSP) as well as the inferring of sympathetic nerve activity (SNA). In a benchmark dataset with PPG data from 42 highly variable individuals with a wide variety of HR and RSP, we have shown that RSP was accurately detected in around 80 % of all cases, even when varying the SR from originally 300 Hz down to 9 Hz. HR was accurately detected at almost 90 % of all cases under the same conditions. In a second study, we used the data from the presented PPG sensing unit, from 6 individuals that performed paced breathing at 0.25 Hz respectively 15 cpm. Similar accuracy performance was detected for these data as well, with a slightly better performance for the lower SR down to 4 Hz. In both studies, no significant indication of sympathetic nerve activity has been observed, however, this specific topic demands for more detailed research.

While the second study particularly confirmed the feasibility of our approach for the implementation on wearable systems, the first study showed its reliability and accuracy for similar data recorded from real patients without paced respiration. It is important to note, though, that the influence of motion has been excluded in both cases. Next, the approach has to be evaluated in a non-stationary environment and, preferably, with an implementation which already enables long-term recordings in everyday life. The final effectiveness and yield have to be determined with a suitable low-power microcontroller, where the use of advanced filters and more efficient FFT derivatives such as the Goertzel algorithm can further improve performance and energy efficiency.

The recorded datasets used in this paper's studies, along with all python scripts and annotations will be available for download to support reproducibility of our experiments on: http://ubicomp.eti.uni-siegen.de

REFERENCES

[1] R. Rox Anderson and John A. Parrish. 1981. The Optics of Human Skin. *Journal of Investigative Dermatology* 77, 1 (1981), 13–19.

[2] Benhur Aysin and Elif Aysin. 2006. Effect of Respiration in Heart Rate Variability (HRV) Analysis. In *Engineering in Medicine and Biology Society, 2006. EMBS'06. 28th annual international conference of the IEEE*. IEEE, 1776–1779.

[3] Peter H. Charlton, Timothy Bonnici, Lionel Tarassenko, Jordi Alastruey, David A. Clifton, Richard Beale, and Peter J. Watkinson. 2017. Extraction of Respiratory Signals from the Electrocardiogram and Photoplethysmogram: Technical and Physiological Determinants. *Physiological Measurement* 38, 5 (2017), 669.

[4] Peter H. Charlton, Timothy Bonnici, Lionel Tarassenko, David A. Clifton, Richard Beale, and Peter J. Watkinson. 2016. An Assessment of Algorithms to Estimate Respiratory Rate from the Electrocardiogram and Photoplethysmogram. *Physiological Measurement* 37, 4 (2016), 610.

[5] A Choi and H Shin. 2017. Photoplethysmography Sampling Frequency: Pilot Assessment of How Low Can We Go to Analyze Pulse Rate Variability with Reliability? *Physiological Measurement* 38, 3 (2017), 586.

[6] Changmok Choi, Byung-Hoon Ko, Jongwook Lee, Seung Keun Yoon, Uikun Kwon, Sang Joon Kim, and Younho Kim. 2017. PPG Pulse Direction Determination Algorithm for PPG Waveform Inversion by Wrist Rotation. In *Engineering in Medicine and Biology Society (EMBC), 2017 39th Annual International Conference of the IEEE*. IEEE, 4090–4093.

[7] Elisabetta De Giovanni, Srinivasan Murali, Francisco Rincon, and David Atienza. 2016. Ultra-Low Power Estimation of Heart Rate under Physical Activity Using a Wearable Photoplethysmographic System. In *Proceedings of the 19th IEEE/Euromicro Conference On Digital System Design (DSD 2016)*. IEEE, 553–560.

[8] A. Fusco, D. Locatelli, F. Onorati, G. C. Durelli, and M. D. Santambrogio. 2015. On how to Extract Breathing Rate from PPG Signal Using Wearable Devices. In *Biomedical Circuits and Systems Conference (BioCAS), 2015 IEEE*. IEEE, 1–4.

[9] Ary L. Goldberger, Luis A. N. Amaral, Leon Glass, Jeffrey M. Hausdorff, Plamen Ch. Ivanov, Roger G. Mark, Joseph E. Mietus, George B. Moody, Chung-Kang Peng, and H. Eugene Stanley. 2000. PhysioBank, PhysioToolkit, and PhysioNet. *Circulation* 101, 23 (2000), e215–e220.

[10] Bassem Ibrahim, Viswam Nathan, and Roozbeh Jafari. 2017. Exploration and Validation of Alternate Sensing Methods for Wearable Continuous Pulse Transit Time Measurement Using Optical and Bioimpedance Modalities. In *Engineering in Medicine and Biology Society (EMBC), 2017 39th Annual International Conference of the IEEE*. IEEE, 2051–2055.

[11] Walter Karlen, J. Mark Ansermino, and Georges Dumont. 2012. Adaptive Pulse Segmentation and Artifact Detection in Photoplethysmography for Mobile Applications. In *Engineering in Medicine and Biology Society (EMBC), 2012 Annual International Conference of the IEEE*. IEEE, 3131–3134.

[12] Walter Karlen, Srinivas Raman, J. Mark Ansermino, and Guy A. Dumont. 2013. Multiparameter Respiratory Rate Estimation from the Photoplethysmogram. *IEEE Transactions on Biomedical Engineering* 60, 7 (2013), 1946–1953.

[13] Jing Liu, Yuan-Ting Zhang, Xiao-Rong Ding, Wen-Xuan Dai, and Ni Zhao. 2016. A Preliminary Study on Multi-Wavelength PPG Based Pulse Transit Time Detection for Cuffless Blood Pressure Measurement. In *EMBC 2016*. IEEE, 615–618. https://doi.org/10.1109/embc.2016.7590777

[14] Marek Malik, A. John Camm, et al. 1996. Guidelines; Heart Rate Variability; Standards of Measurement, Physiological Interpretation, and Clinical Use. *European Heart Journal* 17 (1996), 354–381.

[15] Simon C. Malpas. 1998. The Rhythmicity of Sympathetic Nerve Activity. *Progress in neurobiology* 56, 1 (1998), 65–96.

[16] Toshiyo Tamura, Yuka Maeda, Masaki Sekine, and Masaki Yoshida. 2014. Wearable Photoplethysmographic Sensors – Past and Present. *Electronics* 3, 2 (2014), 282–302.

Received June 2018; accepted August 2018